ELSEVIER

Journal of Process Control 13 (2003) 517–523

JOURNAL OF PROCESS CONTROL

www.elsevier.com/locate/jprocont

Nonlinear receding-horizon state estimation for dispersive adsorption columns with nonlinear isotherm

Mazen Alamir[a,*], Jean Pierre Corriou[b,1]

[a] *Laboratoire d'Automatique de Grenoble. UMR CNRS 5528. LAG/ENSIEG BP 46, Domaine Universitaire. 38400 Saint Martin d'Hèeres, France*

[b] *Laboratoire des Sciences du Génie-Chimique, Groupe ENSIC, 1, rue Grandville. BP. 451, 54001 Nancy Cedex, France*

Received 12 February 2002; received in revised form 23 September 2002; accepted 26 September 2002

Abstract

In this paper, a nonlinear receding-horizon estimation scheme is proposed for general nonlinear diffusive binary chromatographic processes. This is done by approximating the concentration profiles over a suitable truncated functional basis. The resulting vector of unknowns is first reduced using available measurements. Then the remaining part is computed by nonlinear optimization. Numerical simulations are proposed to illustrate the efficiency of the proposed scheme.

Keywords: Chromatographic process; Adsorption column; Nonlinear state observer; Nonlinear isotherm; Moving-horizon observer

1. Introduction

Among different separation tools, chromatographic processes gain increasing importance in domains such as food, fine chemicals and pharmaceutical industry where high purities and yields are required. The chromatographic separation principle lies on the different adsorption affinities of the components in a multi-component mixture. Originally, the processes were operated in batch mode and this operation was repeated resulting in a periodic process. Nowadays, the attractive character of continuous processes is realized in the true countercurrent chromatographic process where several chromatographic columns are disposed in series in which the solid and liquid phases move in opposite direction. Practically, this continuous process suffers from several drawbacks including in particular the fast degradation of the solid adsorbent, so that it is preferable to simulate its movement by cyclic switching of the feed stream and of the inlet and outlet ports in the direction of the fluid flow.

Due to its hybrid character including continuous and discrete dynamics, its operational conditions close to the optimum, its great sensitivity to operation parameters and disturbances, the control of the SMB process is complicated and many different strategies have been proposed for various types of separation [2,4,5,8]. Therefore, the estimation of the current concentration profiles within the columns of the plant for its use in the control design becomes mandatory.

In almost all existing estimation schemes, a simplified linear model is used in order to explicitly exploit wave propagation related arguments to decouple the equations for the different species. Output measurements are then used to add corrections to the above simplification-based estimation scheme [6].

In the present paper, a novel approach is proposed that may handle the general coupled non-linear case. More precisely, a general nonlinear equilibrium law is considered yielding a system of coupled nonlinear PDE's where the "wave propagation" related arguments are no more valid and the coupling phenomena take the system away from the ideal scheme classically used.

* Corresponding author. Tel.: +33-4-76-82-63-26; fax: +33-4-76-82-63-88.

E-mail addresses: mazen.alamir@inpg.fr (M. Alamir), corriou@ensic.inpl-nancy.fr (J.P. Corriou).

[1] Tel.: +33-3-83-17-52-13; fax: +33-3-83-17-53-26.

0959-1524/03/$ - see front matter
PII: S0959-1524(02)00099-9

The basic idea in the proposed approach is to choose a suitable space functional basis for the transient concentration profiles to be correctly approximated. The concentration profiles are then looked for as linear combinations of the basis elements. The coefficients of these linear combinations are then obtained by minimizing a weighted sum of the output prediction errors at past sampling instants over some moving-horizon. Fortunately, in the case of the simulated-moving bed, a part of the measurements can be used to form a linear system of constraints that enable the unknown vector to be parameterized in terms of a reduced-size free parameter vector. The latter are then obtained by solving the corresponding reduced-dimension nonlinear optimization problem. It is worth noting that no ODE's are used to approximate the system's behaviour, the output prediction is obtained by integrating the nonlinear PDE's. The functional basis is only used to define the best estimation of the past initial concentration profiles.

The paper is organized as follows: in Section 2, the estimation problem is clearly stated. In Section 3, it is shown how the estimation problem can be written as an optimization problem. Finally, some implementation issues and numerical experiments are reported in Section 4.

2. Problem statement

A simulated-moving-bed (SMB) chromatographic system (see Fig. 1) is obtained by connecting several single chromatographic columns in series to form four functional sections [10,3]. A countercurrent movement of the bed is simulated by periodically switching the inlet and outlet ports in the direction of the fluid stream. The aim of the whole system is to separate the components A and B initially present in the inlet feed stream. In the case of the SMB shown in Fig. 2, component A is recovered at the outlet of Section 1 while component B is recovered at the outlet of Section 3. The flow rates of the fluid stream in the different four sections can be controlled by varying the four independent flow rates: recycle, extract, raffinate and desorbent. Assuming a fast transfer of species A and B between the two phases, the system behaviour in each section may be described by the following PDE's

$$\frac{\partial}{\partial t}\begin{pmatrix} c_A \\ c_B \end{pmatrix} = Q(c_A, c_B)\left[D_{ax}(u)\frac{\partial^2}{\partial x^2}\begin{pmatrix} c_A \\ c_B \end{pmatrix} - u\frac{\partial}{\partial x}\begin{pmatrix} c_A \\ c_B \end{pmatrix}\right] \quad (1)$$

where the c_js ($j \in \{A, B\}$) refer to the concentrations of species j in the liquid, u is the fluid velocity (cm/s) in the

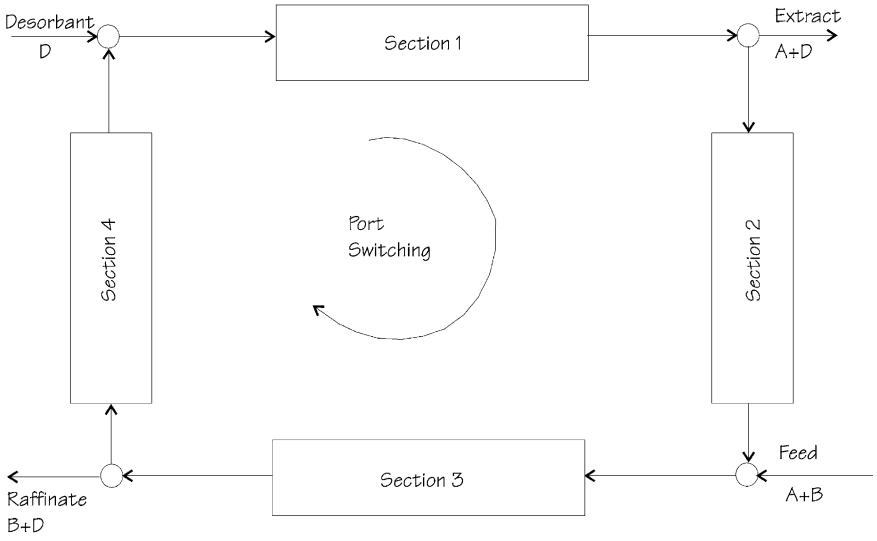

Fig. 1. Schematic view of a simulated moving bed.

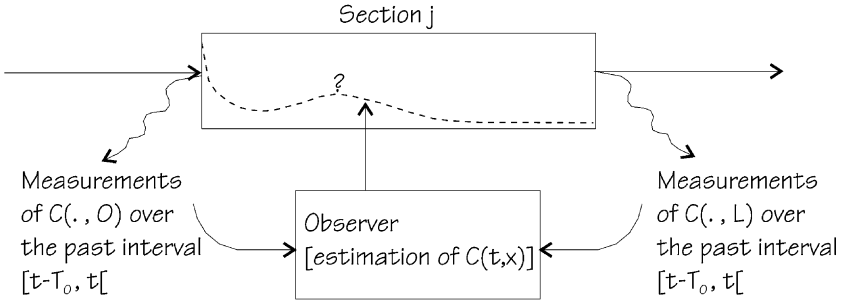

Fig. 2. Definition of the estimation problem.

considered section. ε Is the void fraction and $D_{ax}(u)$ is the dispersion coefficient depending on u according to the following expressions

$$D_{ax}(u) = uL/Pe(u);\ Pe(u) = \frac{2}{\varepsilon} + \frac{0.011}{\varepsilon}\left[\frac{Re(u)}{\varepsilon}\right]^{0.48};\quad Re(u) = \frac{2\varepsilon u R_p \rho}{\eta} \tag{2}$$

where L is the length of the section (cm), Pe is the Peclet number, Re is the Reynolds number, η is the fluid viscosity [g/(cm:s)], R_p is the particle radius (cm) while ρ is the fluid density (g = cm^3). Finally, the matrix $Q(c_A, c_B) \in \mathbb{R}^{2\times 2}$ is given by

$$Q(c_A, c_B) := \begin{pmatrix} 1 + \dfrac{1-\varepsilon}{\varepsilon}\dfrac{\partial q_A^{eq}(c)}{\partial c_A} & \dfrac{1-\varepsilon}{\varepsilon}\dfrac{\partial q_A^{eq}(c)}{\partial c_B} \\ \dfrac{1-\varepsilon}{\varepsilon}\dfrac{\partial q_B^{eq}(c)}{\partial c_A} & 1 + \dfrac{1-\varepsilon}{\varepsilon}\dfrac{\partial q_B^{eq}(c)}{\partial c_B} \end{pmatrix}^{-1} \in \mathbb{R}^{2\times 2} \tag{3}$$

where $q_j^{eq}(c_A, c_B)$ expresses the steady state equilibrium law.

The developments in the present paper hold for arbitrary nonlinear equilibrium relations $q_j^{eq}(c_A, c_B)$. For the concrete simulations of Section 4, however, the following nonlinear Langmuir isotherm is considered

$$q_j^{eq}(c_A, c_B) := \frac{K_j c_j}{1 + K_A c_A + K_B c_B};\quad j \in \{A, B\} \tag{4}$$

Using the row vector $C := (c_A, c_B)$, Eq. (1) becomes

$$\frac{\partial C}{\partial t} = \left[D_{ax}(u)\frac{\partial^2 C}{\partial x^2} - u\frac{\partial C}{\partial x}\right] Q^T(C) \tag{5}$$

To complete the definition of system dynamics, the following boundary conditions are considered [3]

$$C(t, 0) = C^{in}(t);\ \frac{\partial C}{\partial x}(t, 2L) = 0 \tag{6}$$

where $C^{in}(\cdot)$ is some given function of time with values in $\mathbb{R}^2_+$. Note that the original boundary condition on the spatial derivatives in (6) is $\frac{\partial C}{\partial x}(t, \infty) = 0$. However, it has been shown in [3] that this may be replaced by $\frac{\partial C}{\partial x}(t, \alpha L) = 0$ for all $\alpha > 1.3$ without dramatic change in the result. In the following, $\alpha = 2L$ is chosen.

The estimation problem can then be stated as follows (see Fig. 2):

> Based on the PDE's (5) with the boundary conditions (6) describing the dynamics of C in each section, provide an algorithm that uses the measurements of $C(\cdot, 0)$ and $C(\cdot, L)$ over some past time interval $[t-T_O, t[$ to reconstruct the concentration profile $C(t, x)$ at instant t for all $x \in [0, L]$.

Recall that the measured variables are the concentrations $c_j(t, 0)$ and $c_j(t, L)$ ($j \in \{A, B\}$) at the inlet and the outlet of the considered section. Measurements are supposed to be acquired with a sampling rate $\tau > 0$ in order to construct at each instant t, the following two measurement matrices

$$Y^0(t) := \begin{pmatrix} C(t, 0) \\ \vdots \\ C(t-(N_O-1)\tau, 0) \end{pmatrix} \in \mathbb{R}^{N_O\times 2};$$

$$Y^L(t) := \begin{pmatrix} C(t, L) \\ \vdots \\ C(t-(N_O-1)\tau, L) \end{pmatrix} \in \mathbb{R}^{N_O\times 2}$$

Using $Y^0(t)$ and $Y^L(t)$, good approximations of $\dot{Y}^0(t)$ and $Y^L(t)$ may be obtained by measurement pre-conditioning and smooth interpolation. Such approximations will be denoted by $\dot{Y}^0(t) \approx S^{(1)}(Y^0(t))$ and $\dot{Y}^L(t) \approx S^{(1)}(Y^L(t))$ respectively.

The estimation scheme proposed in this work tries to find concentration profiles that belong to the following set

$$\mathcal{A}_c := \left\{f : [0, 2L] \to \mathbb{R}_+ |\ f(x) = B(x)\mu;\ \mu \in \mathbb{R}^{n_a}\right\} \tag{7}$$

where $B : [0;2L] \to \mathbb{R}^{n_a}$ defines a n_a-dimensional twice differentiable functional basis on $[0, 2L]$. With the above definitions, an approximate estimation of $C(t,x)$ is written $C(t, x) \approx B(x)a(t) \in \mathcal{A}_c \times \mathcal{A}_c$ with some $a(t) \in \mathbb{R}^{n_a\times 2}$.

3. The nonlinear observer's design

Given an initial condition $(t_0, C^0) \in \mathbb{R}_+ \times \mathcal{A}_c \times \mathcal{A}_c$ satisfying the boundary conditions (6) at instant t_0, the solution at $t \geqslant t_0$ of (5) under (6) is denoted by $C(t; x; t_0; C^0)$.

Following classical arguments of receding-horizon estimation schemes [1,7,9,11], it may be argued that the estimation of the concentration profiles $C(t, \cdot)$ at instant t amounts to find the optimal estimation $\hat{C}(t - T_O, \cdot)$ of the concentration profile at instant $t - T_O$ and to take $\hat{C}(t, x) = C\left(t; x; t - T_o; \hat{C}(t - T_O, \cdot)\right)$ as an estimation of $C(t,x)$.

Denoting by $B(x)\hat{a}(t)$ the estimate of $C(t - T_O, x)$, one can easily see that $\hat{a}(t)$ has to satisfy the following two 5-dimensional linear system of equations expressing boundary conditions [see the boundary conditions (6) and the system's Eq. (5)].

$$A(t)\hat{a}(t) = b(t)\ ;\ A(t) \in \mathbb{R}^{5\times n_a}\ ;\ b(t) \in \mathbb{R}^{5\times 2}\ ;\ \hat{a}(t) \in \mathbb{R}^{n_a\times 2} \tag{8}$$

where

$$A(t) := \begin{pmatrix} B(0) \\ B(L) \\ B'(2L) \\ D_{ax}(u(t-T_O))B''(0) - u(t-T_O)B'(0) \\ D_{ax}(u(t-T_O))B''(L) - u(t-T_O)B'(L) \end{pmatrix};$$

$$b(t) := \begin{pmatrix} Y^0_{N_O}(t) \\ Y^L_{N_O}(t) \\ 0 \\ S^{(1)}_{N_O}\left(Y^0(t)\right)Q^{-T}\left(Y^0_{N_O}(t)\right) \\ S^{(1)}_{N_O}\left(Y^L(t)\right)Q^{-T}\left(Y^L_{N_O}(t)\right) \end{pmatrix} \tag{9}$$

Therefore, if $n_a = 5$, $\hat{a}(t)$ is clearly given by solving the linear system (8). For higher n_a's, a parameterization of $a(t)$ satisfying (8) is clearly given by

$$a(t) = \bar{a}(v(t)) := A^T(t)\left[A(t)A^T(t)\right]^{-1}b(t) + K(t)v(t); \quad v \in \mathbb{R}^{(n_a-5)\times 2} \tag{10}$$

where the columns of $K(t)$ form a basis for $Ker(A(t))$. Note that $A(t)$ is full rank equal to 5 as $n_a \geqslant 5$ and therefore, the first term in the r.h.s of (10) is nothing but the minimum-norm solution of the linear system $A(t)a(t) = b(t)$.

The estimated profile at instant t is then given by $C(t; x; t - T_O; B(\cdot)\bar{a}(\hat{v}(t)))$ where $\hat{v}(t)$ is given by

$$\hat{v}(t) := \underset{v\in\mathbb{R}^{2(n_a-5)}}{\text{Arg min}} \sum_{\xi\in\{0,L\}} \left\| \begin{pmatrix} C(t;\xi;t-T_O;B(.)\bar{a}(v)) \\ \cdots \\ C(t-(N_O-1)\tau;\xi;t-T_O;B(.)\bar{a}(v)) \end{pmatrix} - Y^{\xi}(t) \right\|^2 \tag{11}$$

Note that the dimension of the decision variable $\hat{v}(t)$ in (11) is $2(n_a - 5)$ instead of $2n_a$ for the original unknown vector $\hat{a}(t)$.

The above formulation offers the possibility for the designer to choose the quality of the approximation used to compute the estimated profiles at each instant t. High values of n_a theoretically lead to better estimation whenever the higher dimensional associated nonlinear optimization problem is correctly solved. Note that the choice $n_a = 5$ corresponds to a free-optimization estimation since in this case, $\hat{a}(t)$ is obtained by a simple solution of the linear system (8).

The preceding development explains how an estimation $\hat{C}(t, x)$ may be obtained using the past measurements $Y^0(t)$ and $Y^L(t)$. The question is how to use the above computation scheme in an on-line estimation context (see Fig. 3).

Note that estimation profiles cannot be available before the instant $t_0 + \Delta t_c$ where $t_0 > (N_O - 1)\tau$ and Δt_c is the computation time needed to solve the optimization problem (11). Indeed, $(N_O - 1)\tau$ instants are first

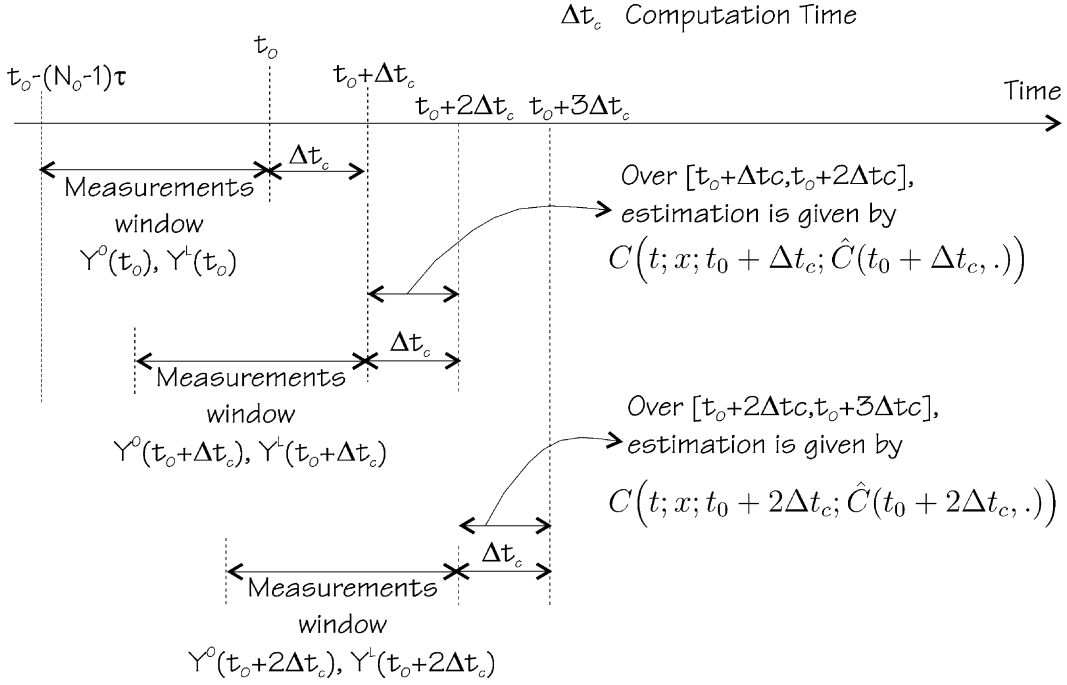

Fig. 3. The on-line observation scheme.

Table 1
Numerical values for simulation [3]

Parameter	Value	Unit	Parameter	Value	Unit
ε	0.45	–	η	0.008	g/(cm s)
K_A	0.56	–	ρ	1	g/cm^3
K_B	0.23	–	R_p	0.0011	cm
L	47.5	cm	u	0.0432	cm/s

required to construct the measurement vectors $Y^0(t_0)$ and $Y^L(t_0)$ then Δt_c time units are needed to solve the optimization problem. Therefore, at instant $t_0+\Delta t_c$, an estimation $\hat{C}(t_0+\Delta t_c, \cdot)$ is obtained. This estimation is used during the computation time (based on the updated measurement vectors $Y^0(t_0+\Delta t_c)$ and $Y^L(t_0+\Delta t_c)$) to continuously obtain an estimation $\hat{C}(t, \cdot)$ for $t \in [t_0+\Delta t_c, t_0+2\Delta t_c]$ and so on.

To sum up, the estimation is obtained continuously based on the estimation $\hat{C}(t_k, \cdot)$ where $t_k = t_0 + k\Delta t_c$. The estimation $\hat{C}(t_k,)$ is updated with a period Δt_c.

4. Numerical experiments

In order to validate the proposed observer, numerical simulations of a SMB's section are necessary in order to obtain the "True profiles" that are compared to the estimated ones. This is done using the subroutine DMOLCH of the IMSL library. This is a general one-dimensional nonlinear PDE's solver. The numerical values of the systems parameters used in the simulation are given in Table 1. The evolution of the concentrations $C^{\text{in}}(.)$ at the section's inlet vs time is depicted in Fig. 4. Note that for $t<200$ s, a simple step is considered, then a wave is created by imposing a decreasing step. This enables a validation of the proposed observer in a somehow "difficult" situation.

When $n_a>5$, nonlinear optimization problem (11) has been solved using the subroutine DBCPOL of the IMSL libraries. Zero-phase forward and reverse digital filtering is first applied to the noisy measurements. Then, the spline interpolation and smoothing subroutine DCSIEZ has been applied to the filtered measurements for the computation of the time-derivatives $S^{(1)}(Y^0(t))$ and $S^{(1)}(Y^L(t))$ necessary to the construction of the linear system (8). A PC-Pentium 600 Mhz has been used and numerical algorithms have been written in DIGITAL FORTRAN 90.

The functional basis used in the definition (7) of approximate profiles is defined as follows

$$B(x) := \left(\exp(-\beta_1 x/L)\ldots, \exp\left(-\beta_{n_a} x/L\right)\right) \in \mathbb{R}^{1\times n_a}$$

where the β_k's are given by

$$\forall k \in \{1, ..., n_a\} \quad \beta_k := \frac{(k-1)\beta_{\max}}{n_a - 1}; \quad \beta_{\max} = 10$$

This choice may be justified by its compatibility with the right-hand boundary conditions and the form of the transient solutions to the system's Eq. (1). The choice of exponential functional basis compared to sinusoidal or polynomial functional basis is motivated by the stiffness of the frontwave. A large value of $\beta_{\max}$ corresponds to stiff variations of the concentration. Also, the β_k's could be optimized as well as the weights but this would increase too much the optimization time.

Noisy measurements have been simulated using the following representation of the relative errors representation of the form

$$y_m(t) = (1 + \varepsilon n(t))y(t) \tag{12}$$

where $n(t) \in [-1, 1]$ is a random number while $\varepsilon = 0.05$ (see Fig. 5).

Several scenarios have been tested corresponding to either stiff rises or stages and for different values of $n_a \in \{5, \ldots, 8\}$ and $N_O \in \{10, 20, 30\}$. Sampling time $\tau = 5$ s has been used. From these simulations, it can be inferred that an execution-time of $\Delta t_c \approx 5$ s is typical when $n_a = 6$ is used, while $\Delta t_c \approx 12$ s and $\Delta t_c \approx 20$ s are typical values for the cases $n_a = 7$ and $n_a = 8$ respectively. Recall that for the

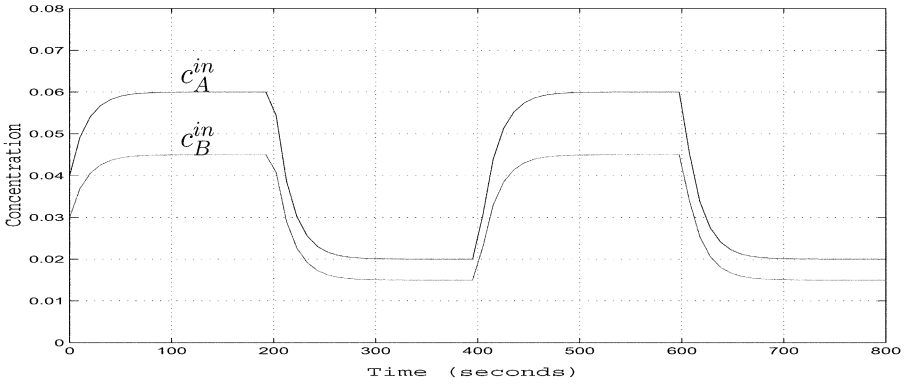

Fig. 4. Time evolution of c_j^{in} at the section's inlet.

particular case $n_a = 5$, computations are quasi instantaneous since only a linear system solution is invoked.

Due to the lack of space and in order to demonstrate the quality of the estimation, only the "worst" results corresponding to a wave being propagating along the section is shown in Figs. 6 and 7 for free-noise (Fig. 6) and noisy measurements (Fig. 7), respectively. The corresponding estimation windows is precisely [212 s; 362 s].

It is worth recalling that the "true profiles" depicted in Figs. 6 and 7 by continuous lines are obtained by

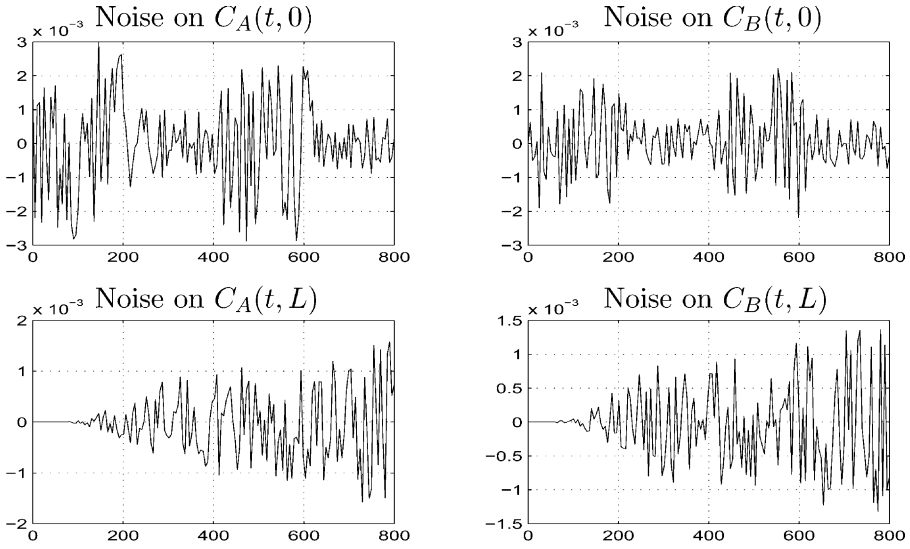

Fig. 5. Measurement noises used in (12) with $\varepsilon = 0.05$.

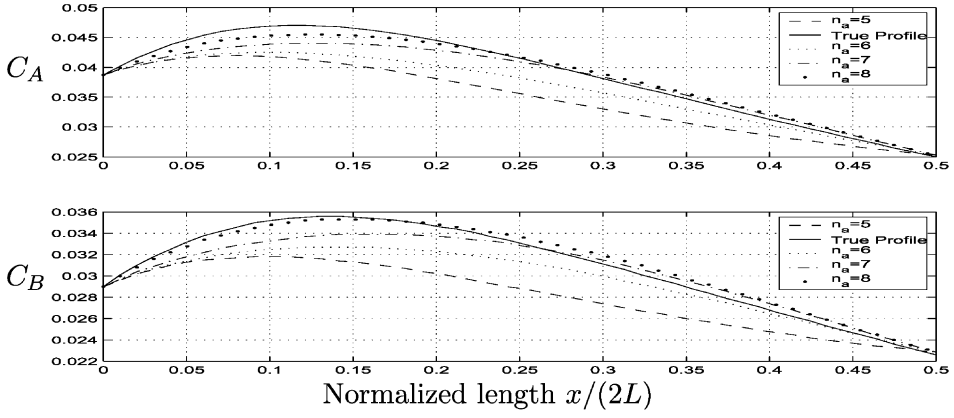

Fig. 6. Estimation based on free-noise measurement for $n_a \in \{5,6,7,8\}$ and $t - T_O = 212$ s.

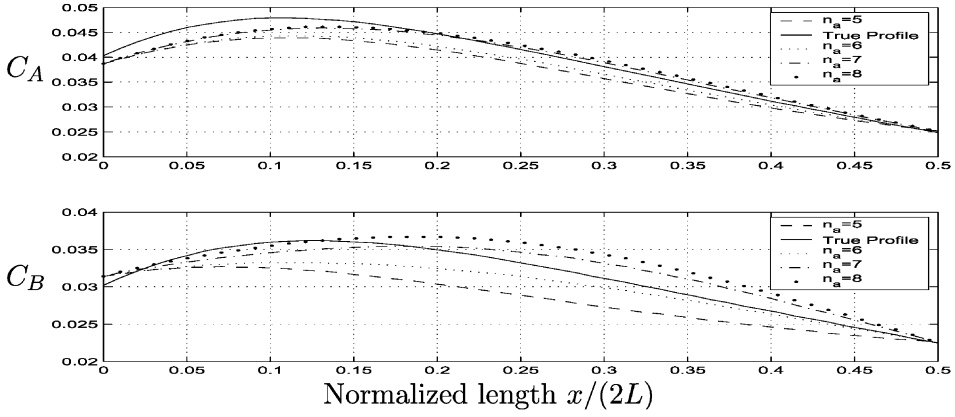

Fig. 7. Estimation based on noisy measurement $n_a \in \{5, 6, 7, 8\}$ and $t - T_O = 212$ s.

integrating the system equations by a direct PDE's solver with 100-points spatial grid and not by using a collocation method based on the n_a-dimensional functional basis $B(x)$. Note finally that the estimated profiles under noisy measurements shown in Fig. 7 are smooth since they represent "shots" at a particular instant and not an evolution (in time) of some estimated variable under noisy measurements as it is usually presented in ODE's related observers.

5. Conclusion

In this paper, an estimation scheme is proposed for the reconstruction of the concentration profiles in a simulated-moving bed based on concentration measurements at the four sections boundaries. The proposed scheme belongs to the family of receding-horizon formulations in which the optimal estimated profile is obtained by minimizing the sum of the squared output-prediction errors at past sampling instants.

A nice feature in the proposed estimation approach is its ability to handle any nonlinear isotherm equilibrium leading to strongly coupled and strongly nonlinear PDE's. When such strong nonlinearities appear, linearization based estimation scheme (the EKF for instance) may theoretically show their limits. Furthermore, the principle is immediately transposable to multi-component chromatographic processes.

References

[1] M. Alamir, Optimization based observers revisited, International Journal of Control 72 (13) (1999) 1204–1217.
[2] M. Benthabet, M. Alamir, M. Bailly, J.P. Corriou. Nonlinear control of a simulated moving bed, in: Proceedings of the AIChE's 1997 Annual Meeting, Los Angeles, 1997, pp. 16–21.
[3] G. Dunnebier, S. Engell, K.U. Klatt, T.H. Schmidt, I. Weirich, Modeling of simulated-moving-bed chromatographic processes with regard to process control design, Computers and Chemical Engineering 22 (9) (1998) 1309–1317.
[4] K.U. Klatt, F. Hanisch, G. Dunnebier, Model-based control of a simulated moving bed chromatographic process for the separation of fructose and glucose, Journal of Process Control 12 (2002) 203–219.
[5] K.U. Klatt, F. Hanisch, G. Dunnebier, S. Engell, Model-based optimization and control of chromatographic processes, Computers and Chemical-Engineering 22 (9) (1998) 1309–1317.
[6] M. Mangold, G. Lauschke, J. Schaffner, M. Zeitz, E.-D. Gilles, State and parameter estimation for adsorption columns by nonlinear distributed parameter state observers, Journal of Process Control 4 (3) (1994) 163–172.
[7] H. Michalska, D.Q. Mayne, Moving horizon observers and observer-based control, IEEE Trans. on Automatic Control 40 (1995) 995–1006.
[8] S. Nataragan, J.H. Lee, Repetitive model predictive control applied to a simulated moving-bed chromatography system, Computers & Chemical Engineering 24 (2–7) (2000) 1127–1133.
[9] L. Robertson, J.B. Rawlings, A moving horizon-based approach for least-squares estimation, AIChE 42 (8) (1996) 2209–2224.
[10] T.H. Schmidt, J. Strube, Dynamic simulation of simulated-moving-bed chromatographic processes, Computers and Chemical Engineering 20 (1996) 641–646.
[11] G. Zimmer, State observation by on-line minimization, Int. Journal of Control 60 (1994) 595–606.